

Technical Notes

TECHNICAL NOTES are short manuscripts describing new developments or important results of a preliminary nature. These Notes cannot exceed 6 manuscript pages and 3 figures; a page of text may be substituted for a figure and vice versa. After informal review by the editors, they may be published within a few months of the date of receipt. Style requirements are the same as for regular contributions (see inside back cover).

Computation of Turbulent Separated Nozzle Flow by a Lag Model

Qing Xiao* and Her-Mann Tsai†

National University of Singapore,

Kent Ridge Crescent 119260, Republic of Singapore

and

Feng Liu‡

University of California, Irvine, California 92697-3975

I. Introduction

SHOCK-INDUCED flow separation can occur in a supersonic overexpanded convergent/divergent (CD) nozzle. Computational simulation of such separated turbulent flow is a challenging task.^{1–4} Turbulence modeling remains a major factor for both the accuracy and efficiency of the computations. Hamed and Vogiatzis^{5,6} computed the flow in an overexpanded CD nozzle and compared the results using several turbulence models. Their results indicate significant spread of the computed shock location and pressure distribution by the different algebraic and two-equation turbulence models. Turbulent separated flows induce nonequilibrium effects, which are not accounted for in low-order turbulence models including the baseline $k-\varepsilon$ and $k-\omega$ turbulence models. More complex Reynolds stress models require large computational resources. Hunter³ and Carlson⁴ used a NASA Langley Reynolds-averaged Navier–Stokes computational fluid dynamics code (PAB3D) to calculate such flows. They used two-equation $k-\varepsilon$ turbulence closure with a nonlinear algebraic Reynolds stress (ARS) model. Their computational results in general agree well with experimental data but the method is still relatively complex and presents numerical stiffness, which may require very fine grid resolution and much computation. To account for the nonequilibrium effects of turbulence, Olsen and Coakley⁷ proposed a lag model. The idea is to take a baseline two-equation model and couple it with a third (lag) equation to model the nonequilibrium effects for the eddy viscosity. Xiao et al.⁸ incorporated the lag model with the baseline $k-\omega$ turbulence model and conducted turbulent simulations for steady and unsteady diffuser flows. Their computational results show significant improvements over results without the lag model for separated flow cases. Compared to the ARS model, the implementation of the lag model on top of a conventional two-equation model requires little change in the computer code because the same numerical algorithm can be used to solve the added lag equation, which is simpler than the other turbulence-model equa-

tions and presents no special numerical difficulties. The objective of the present Note is to explore and document further the capability of the lag model for shock-induced separated flows in supersonic nozzles. The experimental test by Hunter³ of a two-dimensional axisymmetric CD nozzle is used as a benchmark. Comparisons of the computations with and without the lagged equations are presented.

II. Lag Model and the Numerical Method

The details of the computational equations and the numerical method are described by the authors in Ref. 8. The Reynolds-averaged Navier–Stokes equations and the baseline Wilcox⁹ $k-\omega$ turbulence model are used to predict the equilibrium eddy viscosity ν_{tE} . The actual turbulent eddy viscosity used to calculate the Reynolds stress ν_t is expressed by the lag model from Olsen and Coakley⁷ as

$$\frac{\partial}{\partial t}(\rho \nu_t) + \frac{\partial}{\partial x_j}(\rho u_j \nu_t) = a(R_T)\omega\rho(\nu_{tE} - \nu_t) \quad (1)$$

$$a(R_T) = a_0 \left[\frac{(R_T + R_{T0})}{(R_T + R_{T\infty})} \right] \quad (2)$$

where $a_0 = 0.35$, $R_{T0} = 1$, $R_{T\infty} = 0.01$, $R_T = \rho k / \mu_T \omega$, ρ is the density, and ω is the specific dissipation rate.

As Olsen and Coakley⁷ pointed out, the conventional one- and two-equation turbulence models generate Reynolds stresses that respond too rapidly to changes in mean flow conditions partially due to the need to accurately reproduce equilibrium flows. As a result, these baseline turbulence models give unsatisfactory results for flows with significant separation under adverse pressure gradients or across shock waves. The preceding lag equation is essentially a relaxation model intended to account for memory effects of the turbulence eddy viscosity in adjusting to its local equilibrium value. Compared to the ARS model, which is regarded as an intermediate model between two-equation models and Reynolds stress models for improving turbulence modeling at a reasonable computational cost, the lag equation as shown in Eq. (1) is easily coupled with the Navier–Stokes and the $k-\omega$ equations in a time-marching method and has a stable numerical property. The finite volume numerical method for solving the governing equations and the turbulence model equations are described in detail by Liu and Ji¹⁰ and Xiao et al.⁸ The code uses a dual time-stepping method proposed by Jameson¹¹ for unsteady flows. However, for the cases studied in this Note, only the steady option of the code is used. Local time stepping, residual smoothing, and multigrid techniques are used to accelerate the solution for the Navier–Stokes and turbulence model equations.

III. Computational Results and Discussion

The same planar two-dimensional CD nozzle tested and computed by Hunter³ is studied here. Computations are conducted and compared with the experimental data from Ref. 3 for nozzle pressure ratios (NPRs, defined as the ratio of inlet total pressure to static pressure outside the nozzle) between 1.4 and 8.78. The computational domain includes the domain inside the nozzle and an ambient region around the outer surface and downstream of the nozzle. The ambient region extends 30 throat heights downstream of the nozzle exit, 25 throat heights upstream of the nozzle exit, and 25 throat heights normal to the jet axis. Figure 1 shows a close-up view of the grid. For a

Received 10 June 2004; revision received 16 September 2004; accepted for publication 20 September 2004. Copyright © 2004 by the authors. Published by the American Institute of Aeronautics and Astronautics, Inc., with permission. Copies of this paper may be made for personal or internal use, on condition that the copier pay the \$10.00 per-copy fee to the Copyright Clearance Center, Inc., 222 Rosewood Drive, Danvers, MA 01923; include the code 0748-4658/05 \$10.00 in correspondence with the CCC.

*Research Scientist, Temasek Laboratories.

†Principal Research Scientist, Temasek Laboratories. Member AIAA.

‡Professor, Department of Mechanical and Aerospace Engineering, Associate Fellow AIAA.

Reynolds number based on the throat height of 3.2 million, the minimum first grid point from the wall gives a $y^+ < 1$. Grid-dependence tests are performed on three different grids consisting 2432×256 , 1216×128 , and 608×64 grid points, respectively. Computed wall pressure distributions on the three grids (not shown here) indicate that the results on the medium grid almost coincide with those on the fine grid. Therefore, the results on the 1216×128 grid will be shown below. The total pressure and total temperature at the inlet are set to be $p_t = \text{NPR} \times p_a$, $T_t = T_a$, respectively, where p_a is the ambient pressure equal to 14.85 psi and T_a is the ambient temperature set at 530 R. The computational time for one typical case with the lag model is about 6–7% more compared to the time without the lag model. The convergence histories for mass, momentum, and energy are almost the same as those using the baseline model.

A. Pressure Distribution

Figure 2 shows the computed top wall pressure distribution for NPR from 1.4 to 8.78 along with the experimental data. The pressures are normalized by the nozzle inlet total pressure. Significant differences exist between the computational results and the experimental data for NPR values less than 2.4. Hunter³ found the same behavior in his two-dimensional computations and pointed out that the differences were due to the fact that the flow became very three-dimensional at the low NPR values. With increasing NPR, the results with the lag model agree very well with the experiments. A close-up view of the pressure distribution for NPR = 2.4 is shown in Fig. 3 along with Hunter’s computational result with the $k-\epsilon$ ARS model by Shih et al.¹² The lag model accurately predicts the pressure distribution and shock location. However, the baseline $k-\omega$ model without the lag model significantly miscalculates the shock loca-

tion. For $\text{NPR} \geq 5.4$, the flow inside the nozzle becomes essentially shock free. Figure 2 shows that both solutions collapse onto one curve and agree well with the experimental data. The effect of the lag model on the wall pressure is insignificant in those cases.

B. Mach Contours

The computed Mach contours at $\text{NPR} = 2.4, 3.8,$ and 5.4 are shown in Figs. 4a, 4b, and 4c, respectively. The top portion of each of the figures shows the solution without the lag model and the bottom portion is the solution with the lag model for the same flow condition. A well-defined lambda shock appears inside the nozzle for $\text{NPR} = 2.4$. The shock induces a separation on the wall. The flow downstream of the shock is fully detached. At $\text{NPR} = 3.8$, the shock wave moves downstream along the wall toward the exit. The lambda shock system becomes a single oblique shock. However, the shock wave still originates from the inside wall of the nozzle very close to the exit and the flow separates after the shock. As the NPR is further increased to 5.4, the oblique shock moves completely outside the nozzle and the corresponding pressure distribution shown in Fig. 2 indicates that the internal nozzle is shock free. It is seen that the shock locations predicted by the baseline $k-\omega$ model and with the lag model are significantly different for the two cases of the lower NPR values.

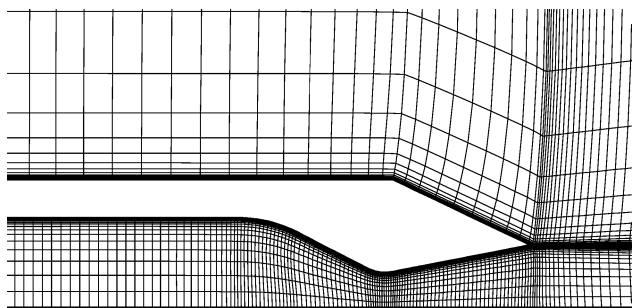


Fig. 1 Grid distribution for the nozzle, 1216×128 mesh (for clarity, only every fifth grid line is drawn in each direction).

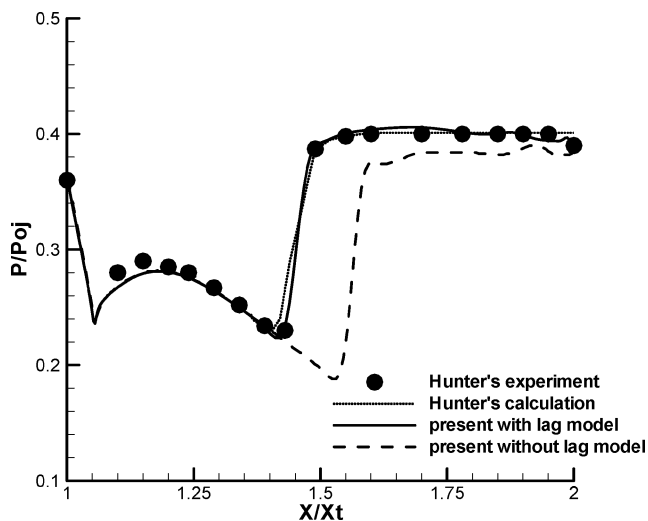


Fig. 3 Comparison of pressure distribution for $\text{NPR} = 2.4$.

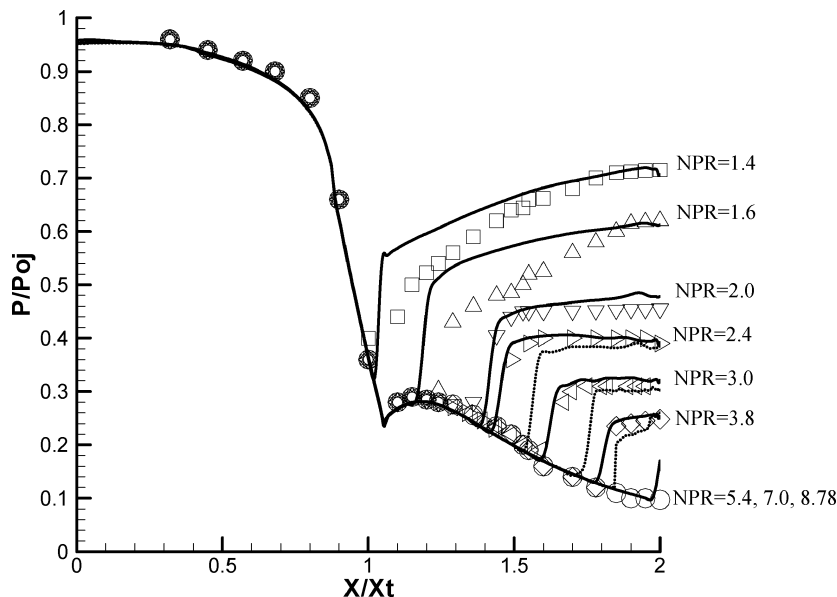


Fig. 2 Comparison of calculated pressure distribution with experimental data³ (symbols, experiment; solid lines, calculation results with the lag model; dotted lines, calculation results without the lag model).

Table 1 Comparison of shock structure

Condition	α_1 , deg	α_2 , deg	α_3 , deg	β_1 , deg	β_2 , deg	M_1	M_2	M_3	$\Delta y/X_t$	X_s/X_t
Experiment	11	0	4	52	73	1.62	1.22	1.02	0.167	1.68
Ref. 3	11	-12	0	52	76	1.6	1.3	1.0	0.114	1.682
Present with lag model	11	-8	1	54	74	1.6	1.27	1.0	0.132	1.676
Present without lag model	11	-8.5	1	54	74	1.6	1.29	1.08	0.132	1.82

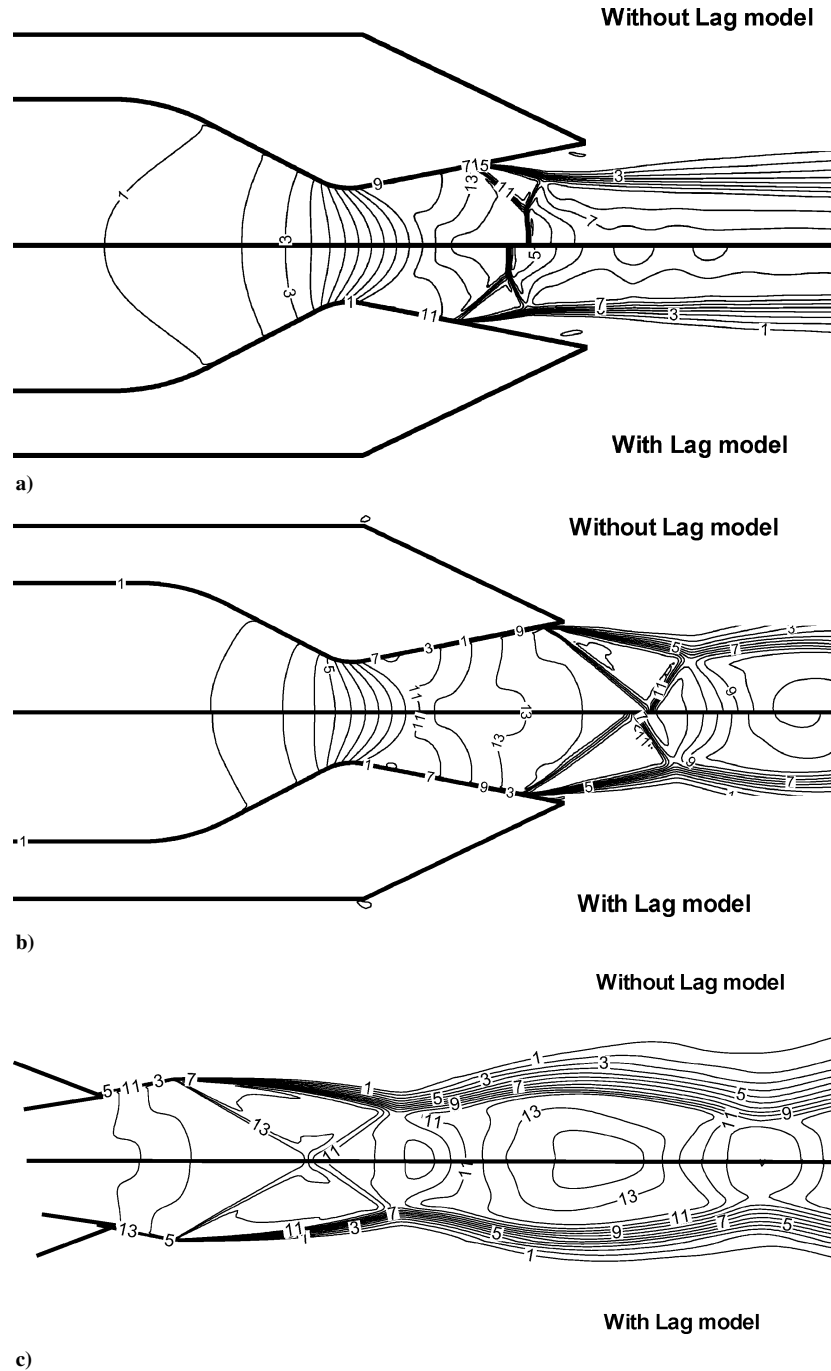


Fig. 4 Mach contours with lag and without lag model: a) NPR = 2.4, b) NPR = 3.8, and c) NPR = 5.4 (maximum value = 1.91, minimum value = 0.15, and interval = 0.3).

C. Shock Structure

The computed shock structure at NPR = 2.4 is analyzed. The corresponding schematic of the shock pattern is illustrated in Fig. 5, where M and α are the flow Mach number and angle, respectively. Subscripts 1, 2, and 3 denote the conditions immediately before and after the first leg of the shock, and that immediately after the second leg of the lambda shock, respectively; $\Delta y/X_t$ is the height of the Mach stem (normal shock) and X_s/X_t is its location, where

X_t is the nozzle throat height. Comparisons of these parameters are made in Table 1 among the experimental data, computations by Hunter in Ref. 3, and the present computations with and without the lag model. The lagged $k-\omega$ model gives the closest M_2 to the experimental value. The predictions of normal shock height by the present computations with and without the lag model are better than that from Ref. 3. The lag model predicts a much better shock location than the baseline without the lag model, close to that reported in

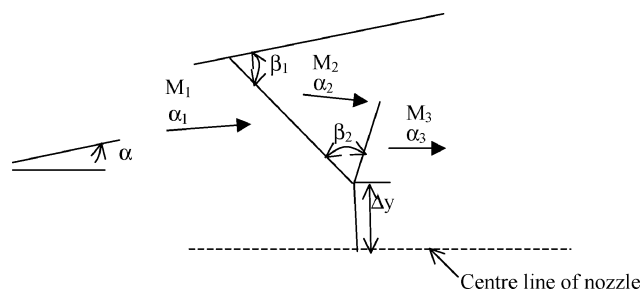


Fig. 5 Shock schematic.

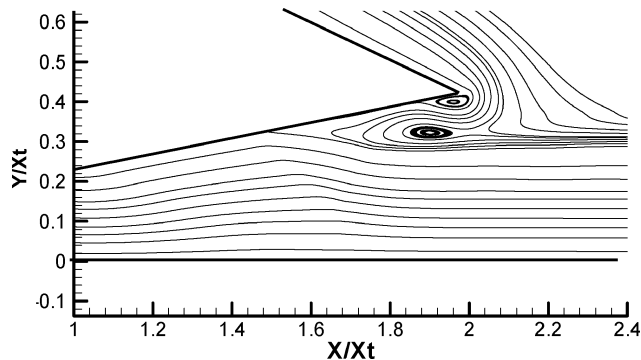


Fig. 6 Streamlines near the rear part of nozzle for $NPR = 2.4$.

Ref. 3. Figure 6 shows the streamline pattern of the flow near the exit of the nozzle for this flow condition. The double-eddy recirculation region is also observed by Hunter in Ref. 3.

The baseline $k-\omega$ turbulence model generates Reynolds stresses that respond too fast to the changes in the mean flow. This problem is severe when the flow is in a nonequilibrium region, such as in the shock-induced separation region of the preceding nozzle flow for $NPR = 2.4$. This is reflected by a large eddy viscosity predicted in the separated area by the baseline model. The lag model effectively reduces the response time of the Reynolds stresses, or rather the values of the turbulent eddy viscosity in this case, through the use of the relaxation model shown in Eq. (1). It better reflects the physics of separated flow and thus yields more accurate results compared to the baseline model.

IV. Conclusions

A computational study of turbulent separated nozzle flow has been conducted using the baseline $k-\omega$ turbulence model with and without the inclusion of a lag model. Results are compared to experimental and computational data using an ARS model. The lag model introduces history effect and relaxation of the eddy viscosity over the equilibrium values predicted by the baseline model. The inclusion of the lag model significantly improves the results where there is strong shock-induced separation. For flows with weak or no separation, the lag model reverts to the baseline model. The lag model provides an attractive engineering alternative to the more complex ARS model.

References

- Asbury, S. C., Gunther, C. L., and Hunter, C. A., "A Passive Cavity Concept for Improving the Off-Design Performance of Fixed-Geometry Exhaust Nozzles," AIAA Paper 96-2541, July 1996.
- Hunter, C. A., "An Experimental Analysis of Passive Shock-Boundary Layer Interaction Control for Improving the Off-Design Performance of Jet Exhaust Nozzles," M.S. Thesis, Dept. of Mechanical and Aerospace Engineering, George Washington Univ., Sept. 1993.
- Hunter, C. A., "Experimental, Theoretical, and Computational Investigation of Separated Nozzle Flows," AIAA Paper 98-3107, July 1998.
- Carlson, J. R., "A Nozzle Internal Performance Prediction Method," NASA TP 3221, 1992.
- Hamed, A., and Vogiatzis, C., "Over-Expanded Two-Dimensional-Convergent-Divergent Nozzles, Assessment of Turbulence Models," *Journal of Propulsion and Power*, Vol. 13, No. 3, 1997, pp. 444-445.
- Hamed, A., and Vogiatzis, C., "Over-Expanded Two-Dimensional-Convergent-Divergent Nozzles, Effect of Three-Dimensional Flow Interactions," *Journal of Propulsion and Power*, Vol. 14, No. 2, 1998, pp. 234-240.
- Olsen, M. E., and Coakley, T. J., "The Lag Model, a Turbulence Model for Non-Equilibrium Flows," AIAA Paper 2001-2564, June 2001.
- Xiao, Q., Tsai, H. M., and Liu, F., "Computation of Transonic Diffuser Flows by a Lagged $k-\omega$ Turbulence Model," *Journal of Propulsion and Power*, Vol. 19, No. 3, 2003, pp. 473-483.
- Wilcox, D. C., "Reassessment of the Scale-Determining Equation for Advanced Turbulence Models," *AIAA Journal*, Vol. 26, No. 11, 1988, pp. 1299-1310.
- Liu, F., and Ji, S., "Unsteady Flow Calculations with a Multigrid Navier-Stokes Method," *AIAA Journal*, Vol. 34, No. 10, 1996, pp. 2047-2053.
- Jameson, A., "Time Dependent Calculations Using Multigrid, with Applications to Unsteady Flows Past Airfoils and Wings," AIAA Paper 91-1596, June 1991.
- Shih, T. H., Zhu, J., and Lumley, J. L., "A New Reynolds Stress Algebraic equation model," NASA TM-106644, Aug. 1994.